Physica Medica 60 (2019) 1–6

Contents lists available at ScienceDirect

Physica Medica

journal homepage: www.elsevier.com/locate/ejmp

Original paper

Evaluating out-of-field doses during radiotherapy of paediatric brain tumours using lead shielding and flattening-filter free beams

Anders Ravnsborg Beierholm[a,*], Ditte Eklund Nygaard[b], Elisabeth Lagoni Juhl[c], Rune Hansen[d], Jolanta Hansen[d]

[a] Danish Health Authority, Radiation Protection, Knapholm 7, DK-2730 Herlev, Denmark
[b] University College Copenhagen, Bachelor's Degree Programme in Radiography, Sigurdsgade 26, DK-2200 Copenhagen, Denmark
[c] Copenhagen University Hospital, Department of Oncology, Blegdamsvej 9, DK-2200 Copenhagen, Denmark
[d] Aarhus University Hospital, Department of Oncology, Palle Juul-Jensens Blvd. 99, DK-8200 Aarhus, Denmark

ARTICLE INFO

Keywords:
Paediatric radiotherapy
Out-of-field dose
Secondary cancer
Lead shielding

ABSTRACT

Paediatric radiotherapy comes at the expense of increased risk of late effects due to out-of-field dose caused not only by the treatment itself but also by image guidance. This study examined how the out-of-field dose to selected radiosensitive organs was affected by applying a 1 mm lead shielding during delivery of volumetric-modulated arc therapy (VMAT) for paediatric brain cancer. The study also investigated how the out-of-field dose to the same organs was affected by the use of flattening-filter free (FFF) beams.

Out-of-field doses to the thyroid, breast and testes were measured using thermoluminescence dosimeters inserted in two anthropomorphic phantoms equivalent to a 1-year and 5-year old child. Coplanar VMAT plans were prepared for 6 MV and 6 MV FFF photon beams and delivered using a Varian TrueBeam linear accelerator, with and without lead shielding applied to the phantoms.

The measured out-of-field doses were as large as 200,9 cGy for the whole treatment, with associated secondary cancer risk being as large as 1,1%. Shielding of the phantoms was found to decrease the out-of-field dose by up to 24%. The use of 6 MV FFF beams yielded a decrease in the dose to the testes by 21–42% compared to 6 MV, while in one case increasing the dose to the thyroid by 18%. The observation that only doses to organs distant to the primary irradiated volume were significantly decreased for FFF can be explained by an increase in internal scatter caused by the softer energy spectrum of the Varian FFF beam.

1. Introduction

In external photon beam radiotherapy, a small fraction of the total delivered dose is deposited outside the primary beam. This out-of-field dose has three causes: leakage radiation from the linear accelerator head, radiation scattered from the collimators of the linear accelerator and radiation scattered internally in the patient. The magnitude and distribution of the out-of-field dose greatly depends on the linear accelerator model, the photon energy spectrum of the primary beam and the radiotherapy technique used [1]. Out-of-field dose calculations can be subject to large inaccuracies, since treatment planning systems are not commissioned for dose calculations far from the penumbra region. A recent AAPM task group report [2] has outlined the various challenges associated with estimating out-of-field doses and the associated risks of late effects such as secondary cancer. As pointed out in the report, any "nontarget" radiation should be minimized as it offers no therapeutic benefit.

Radiotherapy techniques such as volumetric-modulated arc therapy (VMAT) and daily image-guidance procedures have increased treatment delivery precision, improving the therapeutic outcome and the prognosis of the patient. As such, many patients are expected to live long after radiotherapy, increasing the risk of late effects such as secondary cancers. This is especially the case for paediatric patients, who are furthermore characterized by tissues that are more radiosensitive and, depending on the size and location of the target volume, vital organs that may be located closer to the primary beam compared to adults.

The purpose of this study was to evaluate two methods for passively reducing the out-of-field dose to radiosensitive organs for radiotherapy of brain tumours in paediatric patients. The first method concerns the use of lead shielding to reduce the dose from daily image guidance, collimator scatter and head leakage to selected organs out-of-field. This method has been investigated in previous studies, but the reported

* Corresponding author.
E-mail address: anrb@sis.dk (A.R. Beierholm).

https://doi.org/10.1016/j.ejmp.2019.03.008
Received 29 October 2018; Received in revised form 6 March 2019; Accepted 9 March 2019
Available online 20 March 2019

setups and outcomes have varied [3–7]. The second method concerns the use of flattening-filter free (FFF) beams, which are generally reported as yielding lower doses far out-of-field compared to conventional flattened beams [8,9]. However, it is less straightforward how the out-of-field dose is affected closer to the primary beam, where internal scatter and collimator scatter tend to dominate [1,10,11]. The two methods were evaluated by measurements in anthropomorphic phantoms, for two different paediatric ages and two different planning target volume (PTV) sizes.

2. Materials and methods

2.1. Paediatric phantoms and treatment planning

Out-of-field doses to the thyroid, breast and testes were measured using thermoluminescence dosimeters (TLDs) inserted in two anthropomorphic phantoms resembling a 1-year and 5-year old child (CIRS ATOM Dosimetry Phantoms models 704 and 705). Both phantoms were subject to a planning computed tomography (CT) scan, and relevant intracranial anatomic structures were contoured by a radiation oncologist. Coplanar double-arc VMAT plans (6 MV and 6 MV FFF x-rays) were prepared in Varian Eclipse 13.7 mimicking post-operative radiotherapy of an ependymoma situated in the posterior fossa. For each phantom, plans were made for two different spherical sizes of CTV (2 cm and 5 cm diameter) to acknowledge the dependence of target size on out-of-field dose. The CTV-to-PTV margin was 3 mm in all cases. The planned total dose was 54 Gy to the PTV, delivered in 30 fractions. The clinical equivalence of the 6 MV and 6 MV FFF plans was validated by comparing the plan conformity index (see Table 1).

2.2. Lead shielding

Lead shielding of 1 mm thickness was applied to cover the torso of each phantom using lead rubber sheets from decommissioned lead aprons (Mavig Multiplex). A strip of shielding 2.5 cm wide was lightly wrapped around the neck of the phantom (slice 8) to attenuate scattered radiation entering laterally through the gap between the phantom and the primary lead shielding. Furthermore, a 1 mm thick rectangular lead plate was sandwiched between the treatment couch and the phantom, in order to shield the phantom from the posterior side (see Fig. 1). The lead equivalent thickness of the shielding was 1 mm, which was verified by transmission measurements using a Medira 2000 x-ray generator and an Unfors RaySafe x-ray detector, comparing transmission measurements at 100 kVp with tabulated analytical values [12]. The lead shielding was not included in treatment planning or optimization.

2.3. Irradiations and dose measurements

The VMAT plans were treatment approved on a Varian TrueBeam linear accelerator. For each phantom, out-of-field dose measurements were performed for small and large PTV, 6 MV as well as 6 MV FFF, with and without lead shielding of the phantom's torso.

Lithium Fluoride-based TLDs (MTS-7, Radcard s.c.) were individually calibrated using a $^{90}Sr/^{90}Y$-based Mirion IR-2000 TLD irradiator prior to the measurements and after, in order to account for differences in TLD sensitivity and to mitigate differences in TLD response due to energy dependence. Six TLDs were inserted at each organ location. For the 1-year phantom, the thyroid position was defined as being in slice number 9. For the breast, TLDs were placed in the left side of slice number 11, while TLDs for the testes measurements were placed in slice number 20. For the 5-year phantom, the corresponding locations for the thyroid, breast (left side) and testes were in slice number 9, 12 and 25, respectively. In all cases, it was ensured that TLDs and lead shielding was outside of the primary beam.

It was verified that the daily output of the linear accelerator was within 2% of the output at calibration at the time of the measurements. Prior to each irradiation, the phantom was approximately aligned on the treatment couch using the in-room lasers. A cone-beam computed tomography (CBCT) scan of the phantom was then acquired (half fan, 200 degrees posterior scan mode, 100 kV and 150 mAs), followed by a match on bony anatomy and then a couch shift to precisely position the phantom. The phantom and inserted TLDs were then irradiated by delivering a total of three treatment fractions (1.8 Gy each) along with two additional CBCT scans. In this way, the dose to the TLDs realistically corresponded to three full treatment fractions including daily image guidance. During the entire measurement session, 10 TLDs were situated in the treatment control room to quantify the background signal accumulated throughout the duration of the measurements. After irradiation, the doses to all the TLDs were read using a Mirion RE-2000A TLD reader. The measured doses were multiplied by 10 to correspond to the total treatment dose (30 fractions).

2.4. Quantifying back-scatter from the lead shielding

To assess whether radiation back-scattered from the lead shielding could have an impact on the measured dose, a simplified measurement setup was applied with the linear accelerator in Service Mode, delivering a 5 cm × 5 cm non-coplanar 6 MV field posteriorly to the 1-year phantom with the couch at 90 degrees and the gantry at 200 degrees, allowing the primary beam to be as close to the thyroid as possible under clinically plausible conditions. A total of 1000 monitor units were delivered to ensure sufficient dose to the TLDs. Lead shielding was applied to the front of the phantom using the lead blanket, but the lead plate between the phantom and couch was omitted. Dose to the thyroid, breast and testes were then compared with and without the lead blanket.

2.5. Quantifying internal scatter

Additional measurements were made using the 1-year phantom to quantify the relative contribution from internal patient scatter on out-of-field dose. These measurements were made in a manner similar to the ones described above, but with the head of the phantom (slices 1–7) removed. The shoulders of the phantom were aligned with the edge of the couch, and the phantom was then shifted in the cranio-caudal direction so that the primary beam completely avoided the phantom and the treatment couch. This was considered the most optimal setup to minimize the contribution from radiation scattered internally in the phantom and couch. Lead shielding was not applied in this measurement setup. Measurements of dose to the thyroid, breast and testes were then performed to evaluate the relative contribution of internal scatter to the total out-of-field dose for the large PTV 6 MV and 6 MV FFF plans. For these measurements, the phantom was only aligned using the in-room lasers, since a couch shift based on a CBCT match was not possible without the head of the phantom. However, in order to take the imaging dose contribution into account in the comparison, dose measurements without the head of the phantom did also include three CBCT

Table 1
Overview of the conformity index (CI) and number of monitor units (MU) for each treatment plan.

Phantom	PTV	Photon beam	CI	MU
1-year	Small	6 MV	1,261	320
1-year	Small	6 MV FFF	1,259	404
1-year	Large	6 MV	1,199	334
1-year	Large	6 MV FFF	1,173	341
5-year	Small	6 MV	1,289	382
5-year	Small	6 MV FFF	1,286	395
5-year	Large	6 MV	1,185	350
5-year	Large	6 MV FFF	1,178	349

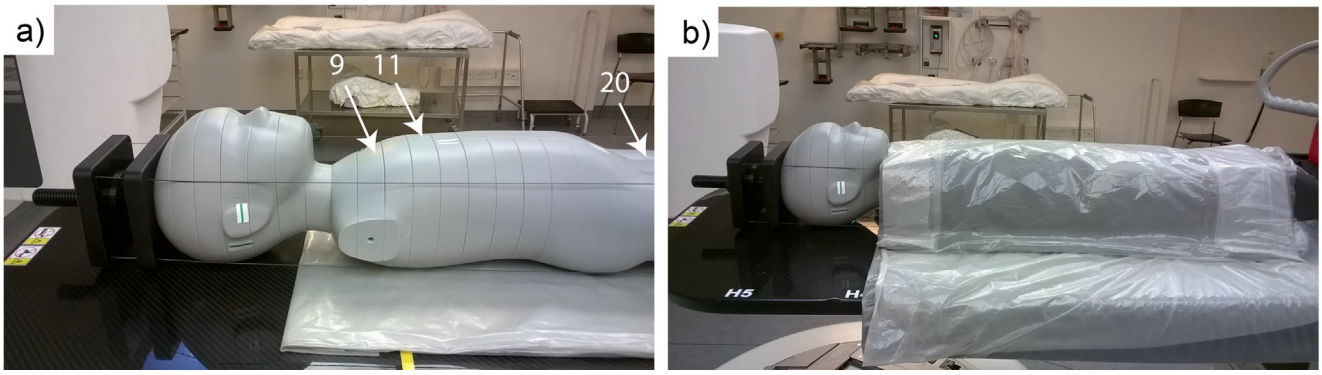

Fig. 1. Lead shielding of the phantoms. a) 1-year phantom positioned with a 1 mm lead plate between the phantom and couch. Slice numbers corresponding to measurement positions are indicated. b) 1-year phantom with a 1 mm lead plate underneath and covered by a 1 mm lead blanket.

scans.

2.6. Data analysis and statistics

"Extreme" outliers in the data set were identified by applying a Tukey's Fence test. Measurements were identified as "extreme" outliers to be excluded from the subsequent data analysis if they deviated from the upper or lower quartile by more than three times the interquartile range. The different irradiation configurations (shielded vs. unshielded, 6 MV vs. 6 MV FFF) were compared and differences were evaluated in terms of statistical significance by applying an unpaired, two-tailed Student's *t*-test with significance level $p < 0,05$. The statistical analysis was performed in IBM SPSS Statistics 25.

2.7. Estimation of secondary cancer risk

The measured out-of-field doses for the conventional, unshielded 6 MV treatments were used to calculate rough estimates of the lifetime attributable risk for cancer incidence, using the sex- age- and organ-specific risk coefficients tabulated in the BEIR VII report [13]. Coefficients were provided for thyroid (male and female) and breast (female). The risk coefficients were used as tabulated, taking into account a dose and dose rate effectiveness factor of 1,5. Since no risk coefficients were provided for 1-year old children, however, the 0-year values were used as conservative estimates.

3. Results

The irradiations resulted in a total of 370 TLD measurements. Out of these, 7 "extreme" outliers were found and excluded from the data analysis.

3.1. Measured organ doses and associated risk of secondary cancer

The measured out-of-field doses for the original 6 MV plans are provided in Table 2 along with estimated risks of secondary cancer for the thyroid and breast. The risks were highest for a 1-year old female, treated using the large-PTV plan, since the BEIR VII risk coefficients are based on a linear dose model and are larger for females than for males and increase with decreasing age [13].

3.2. Comparison of measured doses without and with shielding

Measured organ doses with and without shielding are presented in Fig. 2 for both phantoms and both PTV sizes, reported for the total treatment dose. Shielding of the phantoms for 6 MV yielded a dose reduction for the thyroid between 8% (5-year old, large PTV) and 18% (1-year old, large PTV). For the breast, the dose reduction was between 12% (1-year old, large PTV) and 18% (5-year old, large PTV). For the testes, dose was reduced between 17% (1-year old, large PTV) and 23% (5-year old, small PTV). These dose reductions were all statistically significant ($p \leq 0,02$) except for the thyroid for the large PTV in the 5-year old phantom ($p = 0,09$), which was the case where the thyroid was closest to the primary beam. In the highest-risk case (1-year old female, large PTV), the use of lead shielding was found to reduce the estimated risk of developing a secondary cancer in the thyroid or breast by 0,2%.

Table 2
Measured organ doses and estimated organ-specific risks of secondary cancer for whole treatment (6 MV).

Organ	PTV	Measured dose (mGy)		Sex	Estimated risk (%)	
		1-year old	5-year old		1-year old	5-year old
Thyroid	Small	81,2 ± 2,3	103,4 ± 5,6	Female	0,5	0,4
				Male	0,1	0,1
	Large	172,6 ± 7,4	200,9 ± 9,5	Female	1,1	0,8
				Male	0,2	0,2
Breast	Small	47,2 ± 2,6	40,9 ± 1,8	Female	0,6	0,4
	Large	89,5 ± 6,1	74,5 ± 6,5	Female	1,0	0,7
Testes	Small	6,7 ± 0,2	5,3 ± 0,1			
	Large	12,1 ± 0,3	6,6 ± 0,2			

Comparable results were evident for 6 MV FFF, showing dose reductions between 3% (5-year old, large PTV) and 18% (1-year old, small PTV) for the thyroid, between 10% (1-year old, small PTV) and 21% (5-year old, small PTV) for the breast and between 17% (5-year old, large PTV) and 24% (1-year old, small PTV) for the testes when shielding was applied. Again, results were statistically significant ($p \leq 0,03$) except for the large PTV, 5-year phantom ($p = 0,69$).

Dose measurements for the non-coplanar setup are shown in Table 3. Differences due to frontal lead shielding were within 5 ± 7%, being statistically insignificant ($p \geq 0,18$). This indicates that back-scattered radiation from the lead shielding adds a negligible contribution to the measured out-of-field dose.

3.3. Comparison of measured doses with and without flattening filter

Results for the comparison between 6 MV and 6 MV FFF plans (without shielding of the phantoms) are shown in Fig. 3. Here, dose to the thyroid showed a significant increase of approximately 18% for 6 MV FFF compared with 6 MV for the 1-year phantom, small PTV ($p < 0,01$). In other cases, however, the difference between 6 MV and 6 MV FFF was insignificant ($p \geq 0,12$). Dose to the breast showed a significant decrease of approximately 12% for 6 MV FFF compared with 6 MV for the 5-year phantom, small PTV ($p < 0,01$); other breast doses did not show a significant difference ($p \geq 0,06$). Dose to the testes, however, showed a significant decrease between 21% (1-year old, small

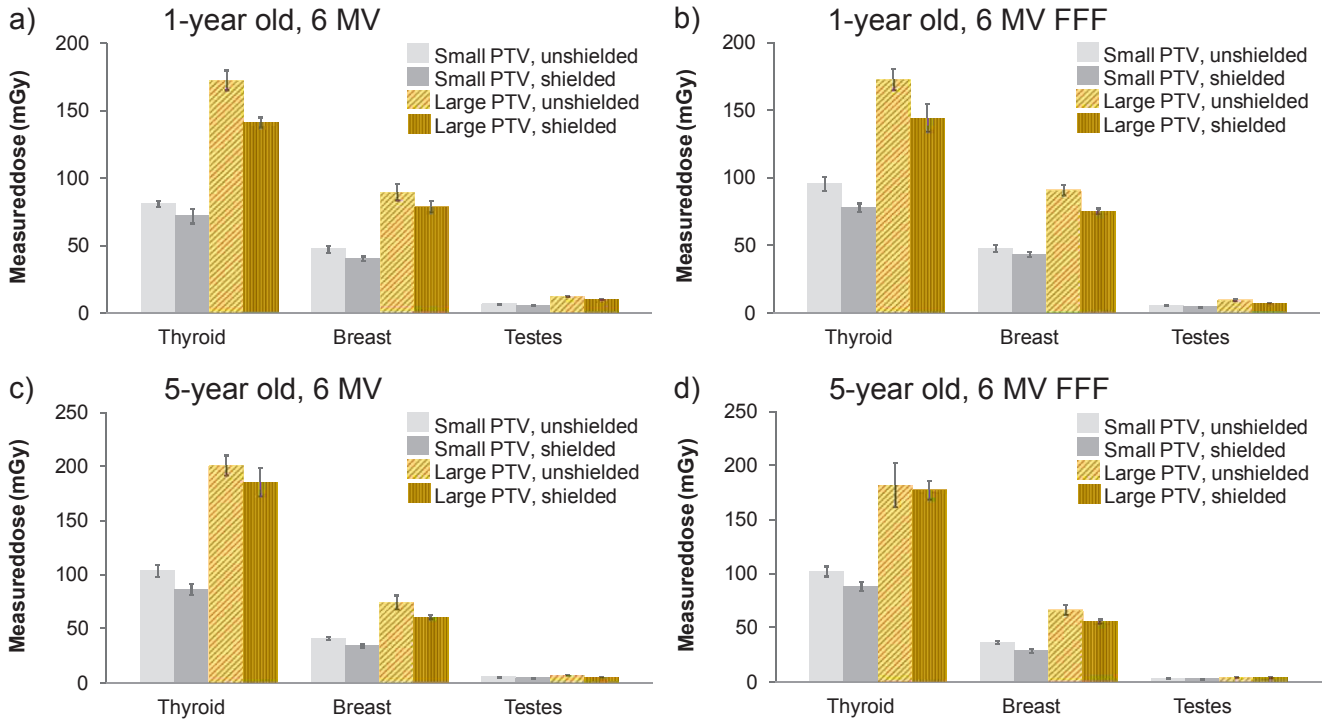

Fig. 2. Measured out-of-field doses for the whole treatment, evaluating the effect of the lead shielding. a) 1-year old (6 MV) with and without shielding, b) 1-year old (6 MV FFF) with and without shielding, c) 5-year old (6 MV) with and without shielding, d) 5-year old (6 MV FFF) with and without shielding. The uncertainty bars indicate two standard deviations of the mean.

Table 3
Measured out-of-field doses for 6 MV non-coplanar irradiation of the 1-year phantom, with and without frontal lead shielding. Uncertainties are given as two standard deviations of the mean.

Organ	Unshielded measured dose (mGy)	Frontal shielding measured dose (mGy)
Thyroid	43,3 ± 1,3	44,7 ± 1,5
Breast	16,2 ± 0,8	17,0 ± 0,8
Testes	1,8 ± 0,0	1,8 ± 0,1

PTV) and 42% (5-year old, small PTV) for 6 MV FFF compared with 6 MV ($p < 0,01$).

3.4. Evaluating the contribution from internal scatter

Doses to all three investigated organs were significantly reduced by 17–37% ($p < 0,01$) for 6 MV FFF compared with 6 MV when removing the head of the 1-year phantom, minimizing the contribution from internal scatter. Comparing the out-of-field dose with and without the head of the 1-year phantom, as shown in Fig. 4, shows that the internal scatter component was as large as 53% for 6 MV and as large as 62% for 6 MV FFF.

4. Discussion

The measured out-of-field doses for the 5-year phantom, large PTV were roughly comparable in magnitude to those reported for IMRT [14] and 3D conformal radiotherapy [15] of intracranial tumours for the same paediatric age. Measured doses were generally higher for the large PTV than for the small PTV for both phantoms. This was assumedly caused by the investigated organs being closer to the primary beam, and by the increase in internal scatter caused by the larger volume irradiated by the primary beam. This further supports the recommendation of using margins as small as reasonably achievable to minimize the primary irradiated volume [4].

Measurements performed on the 5-year phantom suggest that a single CBCT scan is associated with an out-of-field dose of

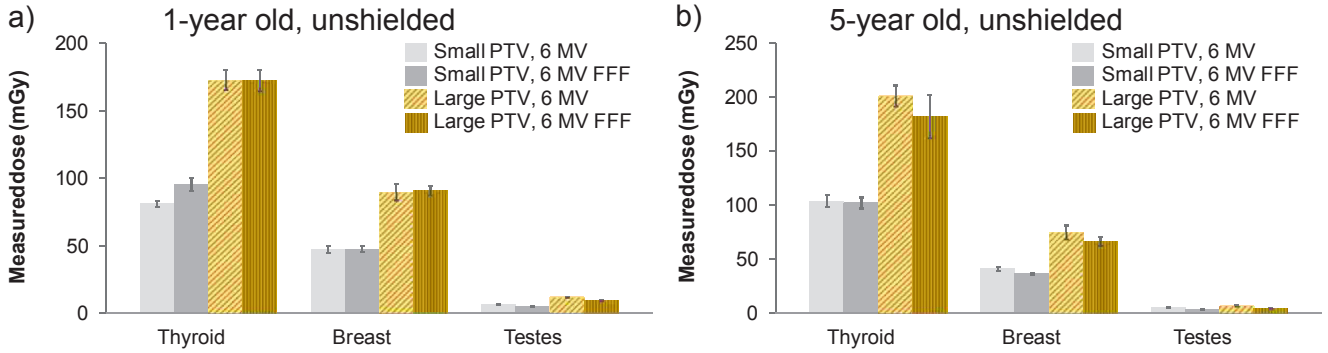

Fig. 3. Measured out-of-field doses for the whole treatment, comparing 6 MV with 6 MV FFF. a) 1-year old, b) 5-year old. The uncertainty bars indicate two standard deviations of the mean.

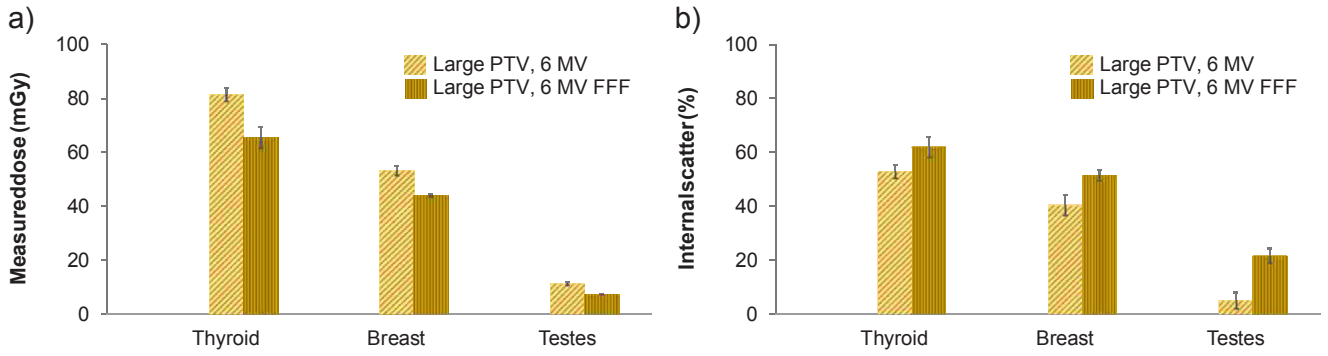

Fig. 4. Measured out-of-field doses for the whole treatment of the 1-year phantom, large PTV, with the head of the phantom removed. a) Comparison between 6 MV with 6 MV FFF, b) Estimated contribution to the total out-of-field dose from internal scatter. The uncertainty bars indicate two standard deviations of the mean.

approximately 0,4 mGy to the thyroid and 0,1 mGy to the breast. The contribution from daily image guidance hereby corresponds to 6–12% of the total out-of-field dose for the thyroid and 5–9% for the breast. By comparison, Hälg, Besserer and Schneider [16] reported an additional out-of-field effective dose contribution of approximately 9% for the Varian CBCT high quality head protocol in conjunction with VMAT treatment. Sung et al. [6] investigated the shielding effect of a 2 mm lead blanket on out-of-field doses from daily CBCT, reporting an out-of-field dose reduction of up to 100% for adult head-and-neck cases. Dose reductions for daily CBCT alone were not investigated in our study, since only the total out-of-field doses from treatment together with imaging were evaluated. However, the transmission measurements performed at 100 kV, as described in Section 2, indicated that most of the out-of-field dose due to CBCT could be blocked using 1 mm lead shielding.

The effect of lead shielding on the total treatment out-of-field dose suggests a clinical possibility to easily reduce the out-of-field dose without compromising treatment efficiency, although the measured dose reductions were not as large as those reported in another recent study. Zhang et al. [6] reported large reductions in the out-of-field dose when applying a 1 mm custom lead shield in an adult phantom study of IMRT for nasopharyngeal carcinoma. The largest dose reductions (as high as 80%) were seen at the surface of the phantom, while measurements performed inside the phantom yielded dose reductions up to approximately 40%. In another recent study, Öğretici et al. [7] reported a 5% reduction in the out-of-field treatment dose by shielding the abdomen with a 0,35 mm lead apron for head-and-neck treatments of pregnant women. For radiotherapy of extracranial paediatric tumours, where the thyroid was located within a few cm from the primary beam, Mazonakis et al. [4] reported dose reductions < 13% for thyroid lead shielding as thick as 5 mm. Taylor, Kron and Franich [3] reported a 50% dose reduction 45 cm from the isocenter, using a lead shielding block of unspecified thickness. These studies are consistent with our findings that although lead shielding yields relatively modest dose reductions out-of-field, it should be considered in the clinical standard of care as a passive, non-invasive tool for radiation protection in adherence to the ALARA principle, at least for paediatric patients. However, the impact of lead shielding on beam hardening and back-scatter should be further explored if a clinical application of the lead shielding is considered.

Comparing the results of the 6 MV and 6 MV FFF VMAT plans show that the doses to organs far from the treatment field (i.e. testes) are reduced for FFF VMAT compared to conventional VMAT, while doses to organs close to the field (in this case, the thyroid) seem to increase, as shown in Fig. 3. Indeed, 26% more MUs were delivered for 6 MV FFF compared to 6 MV in the case of the 1-year old, small PTV. However, the observed increase in dose to the thyroid for FFF was not accompanied by a corresponding relative increase in dose to either the breast or the testes; the difference in dose for breast and testes between 6 MV and 6 MV FFF were consistent between 1-year old, small PTV and 1-year old, large PTV. Therefore, it cannot be concluded that the increase in dose is due to more MUs being delivered for FFF. The observed increase is in line with earlier publications reporting out-of-field doses for FFF beams on Varian linear accelerators [1,10] and can be explained by the softer photon energy spectrum of the FFF beam, which is comparable to a 4 MV rather than a 6 MV beam [17]. The softer spectrum increases the internal scatter component, which tends to dominate the out-of-field dose close to the primary beam. This explanation is further supported by the measurements made for the 1-year phantom with the head removed, which show consistent and significant dose reductions for FFF when the internal scatter component (contributing up to 62%) is minimized. By comparison, Cashmore et al. [11] found that out-of-field doses even 10 cm from the primary beam were consistently decreased when treating intracranial tumours in a 10-year old child using FFF beams on an Elekta linear accelerator, where the photon energy is automatically tuned in FFF mode to match the characteristics of the unflattened 6 MV beam. If a similar energy matching was performed on a Varian linear accelerator, one would therefore assume consistent reductions in out-of-field doses, even in the 1-year and 5-year cases where the relevant organs are located closer to the primary beam.

The estimated risks of secondary cancer were found to be low, but not negligible. Although the risks were only calculated for the two selected organs, other organs of the body (such as the lungs) will also be subject to a low but non-negligible risk. As such, the total risk of secondary cancer, accumulated for all organs listed in the BEIR VII report [13], will be larger than the individual risks listed in Table 2. Furthermore, as pointed out by AAPM TG 158 [2], potential late effects from low doses out-of-field are not limited to secondary cancer risk, but also concern e.g. the risk of cardiovascular toxicity.

5. Conclusions

Application of a 1 mm lead equivalent shielding was shown to systematically decrease the out-of-field dose to the thyroid, breast and testes, for 6 MV as well as 6 MV FFF VMAT plans supported by daily CBCT image guidance. This suggests a clinically relevant application of out-of-field lead shielding in paediatric radiotherapy of brain tumours. A blanket of 1 mm lead equivalent thickness can be considered light enough to be endured by a paediatric patient without the need for additional supporting structures, and it can be easily obtained from commercially available materials. The resulting dose reductions have been shown to reduce the risk of secondary cancer incidence in radiosensitive organs, although by a modest amount.

The comparison of out-of-field doses for clinically equivalent 6 MV and 6 MV FFF VMAT plans indicates that doses to organs far from the primary beam are reduced for FFF, while doses to organs close to the primary beam are in some cases increased. The latter finding can be explained by an increase in internal scatter caused by the softer energy

spectrum of the Varian 6 MV FFF beam. Very young paediatric brain tumour patients are therefore not expected to benefit from lower doses to the thyroid and breast when treated with FFF VMAT, unless the energy spectrum of the 6 MV FFF beam is tuned to match that of the 6 MV beam.

Acknowledgements

This research did not receive any specific grant from funding agencies in the public, commercial, or not-for-profit sectors.

Conflict of interest.

None to disclose.

References

[1] Hälg RA, Besserer J, Schneider U. Systematic measurements of whole-body dose distributions for various treatment machines and delivery techniques in radiation therapy. Med Phys 2012;39:7662–76.
[2] Kry SF, Bednarz B, Howell RM, Dauer L, Followill D, Klein E, et al. AAPM TG 158: Measurement and calculation of doses outside the treated volume from external-beam radiation therapy. Med Phys 2017;44:e391–429.
[3] Taylor ML, Kron T, Franich RD. Assessment of out-of-field doses in radiotherapy of brain lesions in children. Int J Radiat Oncol 2011;79:927–33.
[4] Mazonakis M, Kourinou K, Lyraraki E, Varveris H, Damilakis J. Thyroid exposure to scattered radiation and associated second cancer risk from paediatric radiotherapy for extracranial tumours. Rad Prot Dosim 2012;152:317–22.
[5] Zhang S, Jiang S, Zhang Q, Lin S, Wang R, Zhou X, et al. Reduction in stray radiation dose using a body-shielding device during external radiation therapy. J Appl Clin Med Phys 2017;18:206–13.
[6] Sung J, Baek TS, Yoon M, Kim DW, Kim DH. Estimate of the shielding effect on secondary cancer risk due to cone-beam CT in image-guided radiotherapy. J Korean Phys Soc 2014;65:757–62.
[7] Öğretici A, Çakir A, Akbaş U, Köksal C, Kalafat U, Tambaş M, et al. A phantom study on fetal dose reducing factors in pregnant patients with breast cancer during radiotherapy treatment. J Med Phys 2017;42:128–32.
[8] Xiao Y, Kry SF, Popple R, Yorke E, Papanikolaou N, Stathakis S, et al. Flattening filter-free accelerators: a report from the AAPM Therapy Emerging Technology Assessment Work Group. J Appl Clin Med Phys 2015;16:12–29.
[9] Budgell G, Brown K, Cashmore J, Duane S, Frame J, Hardy M, et al. IPEM topical report 1: guidance on implementing flattening filter free (FFF) radiotherapy. Phys Med Biol 2016;61:8360–94.
[10] Kry SF, Vassiliev ON, Mohan R. Out-of-field photon dose following removal of the flattening filter from a medical accelerator. Phys Med Biol 2010;55:2155–66.
[11] Cashmore J, Ramtohul M, Ford D. Lowering whole-body radiation doses in paediatric intensity-modulated radiotherapy through the use of unflattened photon beams. Int J Radiation Oncology Biol Phys 2011;80:1220–7.
[12] Sutton DG, Martin CJ, Williams JR, Peet DJ. Radiation Shielding for Diagnostic Radiology. The British Institute of Radiology; 2012.
[13] National Research Council. Health Risks from Exposure to Low Levels of Ionizing Radiation: BEIR VII – Phase 2. Washington: National Academies Press; 2007.
[14] Kourinou KM, Mazonakis M, Lyraraki E, Stratakis J, Damilakis J. Scattered dose to radiosensitive organs and associated risk for cancer development from head and neck radiotherapy in pediatric patients. Phys Med 2013;29:650–5.
[15] Majer M, Stolarczyk L, De Saint-Hubert M, Kabat D, Knežević Z. Out-of-field dose measurements for 3D conformal and intensity modulated radiotherapy of a paediatric brain tumour. Rad Prot Dosim 2017;176(3):331–40.
[16] Hälg RA, Besserer J, Schneider U. Systematic measurements of whole-body imaging dose distributions in image-guided radiation therapy. Med Phys 2012;39:7650–61.
[17] Vassiliev ON, Titt U, Pönisch F, Kry SF, Mohan R, Gillin MT. Dosimetric properties of photon beams from a flattening filter free clinical accelerator. Phys Med Biol 2006;51:1907–17.